



KEK Preprint 96-19  
 May 1996  
 H

## Measurement of $D^{*\pm}$ production in two-photon processes at TRISTAN

### AMY Collaboration

N. Takashimizu<sup>a</sup>, T. Sasaki<sup>b</sup>, H. Miyata<sup>a</sup>, T. Aso<sup>a</sup>, K. Miyano<sup>a</sup>, N. Nakajima<sup>a</sup>, K. Ohkubo<sup>a</sup>,  
 M. Satou<sup>a</sup>, M. Shirai<sup>a</sup>, Y. Yamashita<sup>c</sup>, K. Abe<sup>b</sup>, Y. Fujii<sup>b</sup>, S. Igarashi<sup>b</sup>, Y. Kurihara<sup>b</sup>,  
 M.H. Lee<sup>b</sup>, F. Liu<sup>b</sup>, A. Maki<sup>b</sup>, T. Nozaki<sup>b</sup>, T. Omori<sup>b</sup>, H. Sagawa<sup>b</sup>, Y. Sakai<sup>b</sup>, Y. Sugimoto<sup>b</sup>,  
 Y. Takaiwa<sup>b</sup>, S. Terada<sup>b</sup>, P. Kirk<sup>d</sup>, T.J. Wang<sup>e</sup>, A. Abashian<sup>f</sup>, K. Gotow<sup>f</sup>, L. Pilonen<sup>f</sup>,  
 S.K. Choi<sup>g</sup>, C. Rosenfeld<sup>h</sup>, L.Y. Zheng<sup>h</sup>, R.E. Breedon<sup>i</sup>, Winston Ko<sup>j</sup>, R.L. Lander<sup>k</sup>,  
 J. Rowe<sup>l</sup>, S. Kanda<sup>l</sup>, S.L. Olsen<sup>l</sup>, K. Ueno<sup>l</sup>, F. Kajino<sup>k</sup>, S. Schnetzer<sup>l</sup>, S. Behari<sup>m</sup>,  
 S. Kobayashi<sup>m</sup>, A. Murakami<sup>m</sup>, S.K. Sahu<sup>m,p</sup>, J.S. Kang<sup>n</sup>, D.Y. Kim<sup>n</sup>, S.S. Myung<sup>n</sup>,  
 H.S. Ahn<sup>o</sup>, S.K. Kim<sup>o</sup>, and S. Matsumoto<sup>q</sup>

<sup>a</sup>*Niigata University, Niigata 950-21, Japan*

<sup>b</sup>*KEK, National Laboratory for High Energy Physics, Ibaraki 305, Japan*

<sup>c</sup>*Nihon Dental College, Niigata 951, Japan*

<sup>d</sup>*Louisiana State University, Baton Rouge, LA 70803, USA*

<sup>e</sup>*Institute for High Energy Physics, Beijing 100039, China*

<sup>f</sup>*Virginia Polytechnic Institute and State University, Blacksburg, VA 24061, USA*

<sup>g</sup>*Gyeongsang National University, Chinju, 660-701, South Korea*

<sup>h</sup>*University of South Carolina, Columbia, SC 29208, USA*

<sup>i</sup>*University of California, Davis, CA 95616, USA*

<sup>j</sup>*University of Hawaii, Honolulu, HI 96822, USA*

<sup>k</sup>*Konan University, Kobe 658, Japan*

<sup>l</sup>*Rutgers University, Piscataway, NJ 08854, USA*

<sup>m</sup>*Saga University, Saga 840, Japan*

<sup>n</sup>*Korea University, Seoul 136-701, South Korea*

<sup>o</sup>*Seoul National University, Seoul 151-742, South Korea*

<sup>p</sup>*National Taiwan University, Taipei, 10764, Taiwan, China*

<sup>q</sup>*Chuo University, Tokyo 112, Japan*

### Abstract

The inclusive cross section for the production of charmed  $D^{*\pm}$  mesons in two-photon processes is measured with the AMY detector at the TRISTAN  $e^+e^-$  collider.  $D^{*\pm}$  mesons are identified from the distribution of charged-particle transverse momenta relative to the jet axis. A data sample corresponding to an integrated luminosity of  $176 \text{ pb}^{-1}$  at a center-of-mass energy of 58 GeV is used to determine a cross section  $\sigma(e^+e^- \rightarrow e^+e^-D^{*\pm}X) = 270 \pm 49(\text{stat}) \pm 38(\text{syst}) \text{ pb}$ . The results are compared with theoretical expectations based on the Vector Meson Dominance, direct quark-parton model, and resolved photon processes.

SCAN-9608096



CERN LIBRARIES, GENEVA

Sw 9634

**National Laboratory for High Energy Physics, 1996**

KEK Reports are available from:

Technical Information & Library  
National Laboratory for High Energy Physics  
1-1 Oho, Tsukuba-shi  
Ibaraki-ken, 305  
JAPAN

Phone: 0298-64-5136  
Telex: 3652-534 (Domestic)  
(0)3652-534 (International)  
Fax: 0298-64-4604  
Cable: KEK OHO  
E-mail: Library@kekvox.kek.jp (Internet Address)

## 1 Introduction

The QCD predictions for the inclusive production of heavy quarks in two-photon collisions are less ambiguous than those for light quark production, making measurements of the former interesting tests of the theory. In heavy quark production, the contributions from Vector Meson Dominance processes (VMD) [1] are small, and only the direct quark-parton model process (QPM) and resolved photon processes [2, 3] need to be considered. The large quark mass insures the validity of perturbative calculations.

In resolved photon processes, one or both of the photons are resolved into partons and one of these partons interacts with the other photon or a parton inside that photon. In calculations of heavy quark production, a free parameter that specifies the minimum transverse momentum cut-off  $P_T^{min}$  for the produced quark, which plays an important role in light quark production, is not needed. Moreover, among the many resolved process diagrams, only the photon-gluon fusion process contributes significantly to heavy quark production.

Studies of charm production in two-photon process have been performed by several groups at lower energies [4]. Recent measurements at TRISTAN [5-9] indicate that the charm production cross sections for small values of the charm-particle transverse momentum are well described as the incoherent sum of the QPM and resolved photon processes including higher-order QCD corrections [10]. However, for larger values of the charm quark transverse momentum, there appears to be some excess over expectations based on these two processes.

A common experimental method for identifying charm quark production relies on detecting  $D^{*+}$  mesons using the  $D^{*+} - D^0$  mass difference. (Throughout the paper the inclusion of charge-conjugate modes is implied.) Recently the TOPAZ group has successfully applied the soft-pion method, previously used in single-photon annihilation processes [11], to two-photon production [7]. This method exploits the very small transverse momentum, relative to the parent  $D^{*+}$  direction, of the “soft” pion ( $\pi_s^+$ ) from the  $D^{*+} \rightarrow D^0\pi_s^+$  decay. This method provides improved statistical precision compared to the mass difference method, where the reconstruction of exclusive  $D^0$  decay modes is required. In this letter, we report a measurement of the two-photon production cross section for high transverse momentum  $D^{*+}$  mesons using the soft-pion method.

## 2 Untag event selection

The results presented here are based on a  $176 \text{ pb}^{-1}$  data sample collected with the AMY detector at the TRISTAN  $e^+e^-$  collider at  $\sqrt{s} = 58 \text{ GeV}$ . Charged particle trajectories are measured by the central drift chamber (CDC) and photons are detected in the barrel (SHC) and endcap (ESC) electromagnetic shower counters. These three devices are located in a 3 Tesla magnetic field. A detailed description of the AMY detector is provided in ref. [12].

For this analysis, events are selected according to the following criteria:

- (1) There are at least four charged tracks originating from within  $r = 4 \text{ cm}$  and  $|z| = 10 \text{ cm}$  of the interaction point, with polar angle in the range  $25^\circ \leq \theta \leq 155^\circ$ . Of these, at least two have  $|p| \geq 0.75 \text{ GeV}/c$  and at least one has  $|p_T| \geq 1.0 \text{ GeV}/c$ .

- (2) The net charge of the observed charged tracks satisfies  $|\Sigma q_i| \leq 2$ .
- (3) The net transverse momentum satisfies  $|\Sigma p_{T,i}| \leq 5.0 \text{ GeV}/c$ , where  $p_{T,i}$  is the projection of the observed momenta on the plane transverse to the beam direction.
- (4) The observed mass of the hadron system  $W_{vis}$  must be between 4 and 20  $\text{GeV}/c^2$ , where  $W_{vis}$  is calculated for charged (assuming a pion mass) and neutral particles (assuming zero mass).
- (5) The most energetic shower cluster appearing in the electromagnetic calorimeters (SHC and ESC) must have an energy less than  $0.25 E_{beam}$ .

The first requirement ensures a high trigger efficiency for accepted events. The charge and transverse-momentum balance requirements eliminate beam-gas and spent-beam-particle induced background events. The  $W_{vis}$  selection eliminates background and single-photon annihilation events. The final requirement, the “anti-tagging” selection, eliminates two photon processes where one photon is highly virtual. A total of 18653 events are selected; these constitute the *untag event sample*.

The experiment utilizes a number of different trigger conditions, none of which are totally redundant. The trigger efficiency is estimated from a comparison of the fractions of events triggered by different sets of individual trigger modes with Monte Carlo expectations. The error is estimated from the variation of the trigger efficiency when different combinations of trigger modes are chosen. In this way, we determine the trigger efficiency to be  $0.90 \pm 0.11$ .

## 3 Monte Carlo simulation

Samples of Monte Carlo events, generated according to the various models discussed in the introduction and processed through a simulation of the AMY detector, are used to determine the trigger efficiency (as described above), determine the detection efficiency, and compare experimental results with theoretical predictions. For the direct QPM process, we use the event generator developed by Kuroda [13] to produce partons that are then evolved into hadrons according to the parton shower scheme [15]. Partons from resolved photon processes are generated according to the formulae given by Drees and Godbole in ref. [3], using the LAC1 parameterization for the distribution of quarks and gluons inside the photon [14]. In all of these calculations, a charm quark mass of  $1.6 \text{ GeV}/c^2$  is used. The produced partons are fragmented into hadronic final states by means of the Lund string fragmentation model as implemented in the JETSET 7.3 program [15] with the PDG [16] values for the  $D^{*+}$  meson branching fractions were incorporated into the decay table. Diffractively produced hadrons are generated using the VMD model. For these events, we use the Field-Feynman fragmentation model with the PLUTO group’s tuned values for the fragmentation parameters. The details of the Monte Carlo simulation are described in ref. [17].

## 4 Analysis of the $p_T^2$ distribution

Since the  $Q$ -value for the  $D^{*+} \rightarrow D^0\pi_s^+$  decay is only 5.8 MeV, the produced pions move very nearly in the parent  $D^{*+}$ ’s line of flight, and their transverse momentum ( $p_T$ ) with

respect to the  $D^{*+}$  direction is much smaller than the typical values for other particles in the event. Thus,  $D^{*+}$  production is reflected as a peak at very small values in the  $p_T^2$  distribution of particles.

The direction of the  $D^{*+}$  is approximated by the direction of the observed jet of hadrons. Charged and neutral tracks detected in the CDC and SHC are clustered into jets in the laboratory frame according to the scaled-invariant-mass algorithm developed by the JADE group [18]. To be accepted as a jet, a cluster is required to have at least three tracks, which eliminates jets with poorly defined jet axes. The transverse momentum and pseudorapidity of the jet relative to the beam direction are required to be  $p_T^{\text{jet}} \geq 2.5$  GeV/c and  $|\eta| \leq 1.0$ , respectively. These requirements tend to reject remnant (spectator) jets from the resolved processes and most VMD-type events.

Figure 1 shows the  $\pi_s^+$  transverse momentum distribution with respect to the beam axis for the simulated QPM events. This distribution was used to determine the selection criteria for the  $\pi_s^+$  candidate tracks. The transverse momentum with respect to the beam axis of the candidate tracks is required to be between 0.2 GeV/c and 0.4 GeV/c; this insures good tracking efficiency and momentum resolution. The opening angle between a track and jet axis is smallest among all tracks in that jet.

The  $p_T^2$  distribution with respect to the jet axis of the selected tracks is shown in Fig. 2(a). A  $D^{*+}$  signal is evident as an enhancement near zero  $p_T^2$  values. The background under the peak, the determination of which is described below, is indicated by the solid line.

In order to estimate the background, we use a function of the form

$$f_1(p_T^2) = a \exp(-bp_T^2) + c,$$

with parameters determined from fits to the  $p_T^2$  distribution of the Monte Carlo (VMD + QPM + LAC1) event sample, excluding  $D^{*+} \rightarrow D^0\pi^+$  decays, over the range  $0 \leq p_T^2 \leq 0.08 \text{ GeV}^2/c^2$ . The results of this fit are shown in Fig. 2(b). The normalization is determined by fitting this function to the experimental data for  $p_T^2$  values for an adjustable range. A number of  $p_T^2$  ranges were used to determine the background normalization, ranging from  $0.02 \leq p_T^2 \leq 0.06 \text{ GeV}^2/c^2$ , to  $0.02 \leq p_T^2 \leq 0.11 \text{ GeV}^2/c^2$ , each giving a similar number of background tracks under the low- $p_T^2$  peak (i.e., for  $p_T^2 \leq 0.012 \text{ GeV}^2/c^2$ ). The solid line in Fig. 2(a) corresponds to the background determined by the fit performed for  $0.02 \leq p_T^2 \leq 0.08 \text{ GeV}^2/c^2$ . We use the average of the results from the different  $p_T^2$  ranges as the background, and include the variance in the systematic error. Subtracting this background from the observed number of tracks in the range of  $p_T^2 \leq 0.012 \text{ GeV}^2/c^2$  gives  $191 \pm 34(\text{stat})$   $D^{*+}$  signal tracks.

The main source of the systematic error is the uncertainty in the background contribution. A 7% systematic error due to the fitting range is assigned as half the difference between the extreme background values. To estimate the uncertainty due to the shape assumed for the background function, we repeated the analysis using the different function,

$$f_2(p_T^2) = \frac{a}{1 + bp_T^2 + c(p_T^2)^3},$$

in which case the number of signal tracks changed by 3%. An error due to the use of different  $p_T^2$  bin widths is determined by varying the bin width between 0.002 and 0.004

$\text{GeV}^2/c^2$ , and it founds out to be negligible. The systematic error due to the uncertainty in luminosity measurements and trigger efficiency calculation are 2% and 12%, respectively. Combining all the errors in quadrature gives a total systematic error of 14% for a final number of  $D^{*+}$ 's of  $191 \pm 34(\text{stat}) \pm 27(\text{syst})$ .

A comparison of the data with the QCD Monte Carlo prediction is shown in Fig. 3. Here we incorporate the effects of next-to-leading order (NLO) QCD terms by multiplying the LO calculation for  $\gamma\gamma \rightarrow c\bar{c}$  by a correction factor of 1.27 and that for  $\gamma g \rightarrow c\bar{c}$  by a correction factor of 2.26. Detailed discussions of these NLO QCD correction factors are given in refs. [5] and [10]. The branching fraction for  $c\bar{c} \rightarrow D^{*+}X$  is taken to be 0.608. Here it is assumed that the ratio of a charm quark fragmenting into a  $D^*$  or a  $D$  is 3 : 1 and that the probability of charm quark going into  $(c\bar{u})$  or  $(c\bar{d})$  is 0.81 [15]. The Monte Carlo simulation predicts a total of  $127 \pm 5(\text{stat})$   $D^{*+}$ 's for our experiment. The QPM and LAC1 contributions are 72% and 28%, respectively. The observed number of  $D^{*+}$ 's is 1.5 standard deviation larger than the VMD + QPM + LAC1 Monte Carlo predictions.

## 5 The $D^{*\pm}$ production cross section

The total cross section of inclusive  $D^{*\pm}$  production is determined from the relation

$$\sigma(e^+e^- \rightarrow e^+e^-D^{*\pm}X) = \frac{N_{\text{obs}}}{\mathcal{L}Br(D^{*+} \rightarrow D^0\pi^+)\varepsilon},$$

where  $N_{\text{obs}}$  is the observed number of signal tracks,  $\mathcal{L}$  is the integrated luminosity, and  $\varepsilon$  is the detection efficiency for the  $D^{*+} \rightarrow D^0\pi^+$  decay mode. The detection efficiency is calculated to be 0.59% using the QPM+LAC1 Monte Carlo simulation. In the calculation we use the charm mass of  $1.6 \text{ GeV}/c^2$  and  $\gamma\gamma$  invariant mass threshold of  $4.0 \text{ GeV}/c^2$ . The total measured cross section, using the QPM+LAC1 model for the acceptance calculation, is

$$\sigma(e^+e^- \rightarrow e^+e^-D^{*\pm}X) = 270 \pm 49(\text{stat}) \pm 38(\text{syst}) \text{ pb}.$$

Here the systematic error does not include the effects due to the uncertainty of the photonic gluon density.

This result is compared to other experiments in Fig. 4. All the data points except for AMY have been obtained using the mass difference method and taken from ref. [19]. The published results in ref. [19] are adjusted for the latest values for  $D^{*+}$  and  $D^0$  branching ratios. The ALEPH data point is obtained using a detection efficiency calculation based on the QPM+GRV model. The curves in the figure are the predictions of the Born level calculation (denoted as QPM in the figure) and the direct plus resolved photon processes with the NLO corrections, where the parton distribution in the photon is taken from the LAC1 and GRV model and the charm quark mass is taken to be  $1.6 \text{ GeV}/c^2$ . As can be seen in the figure, our data point lies above the QCD prediction using the LAC1 parton density, which has a relatively large gluon content, while the ALEPH result lies close to the QCD prediction using the GRV parton density, which has a relatively small gluon content.

We compare our differential cross section measurements with published results. Over the acceptance region covered by the TOPAZ experiment, i.e.,  $p_T^{D^{*+}} \geq 2.6 \text{ GeV}/c$  and

$|\cos\theta| \leq 0.77$ , we estimate a cross section of  $12.4 \pm 2.3(\text{stat})$  pb, which is in agreement with the TOPAZ measurement of  $9.3 \pm 2.2$  pb [7]. In a previous letter, we reported a measurement of the high  $p_t$  charm production cross section based on a study of the rate of inclusive lepton production [5]. The measured transverse momentum range of the  $D^{*\pm}$ ,  $p_t^{D^{*\pm}} \geq 2$  GeV/c, is similar to that for the present experiment. The inclusive-lepton analysis yields a cross section that is 1.8 standard deviations above the QCD prediction and consistent with the result reported here.

## 6 Conclusion

We measured the inclusive cross section of  $D^{*\pm}$  production in quasi-real two-photon processes, using the the transverse momentum distribution of charged particles with respect to the jet axis. The measured cross section  $\sigma(e^+e^- \rightarrow e^+e^-D^{*\pm}X) = 270 \pm 49(\text{stat}) \pm 38(\text{syst})$  pb is 1.5 standard deviations larger than the incoherent sum of the theoretical predictions of the VMD, direct QPM, and resolved photon processes with the LAC1 photonic charm density.

## Acknowledgement

We thank the TRISTAN staff for the excellent operation of the storage ring. We acknowledge the strong support provided by the staffs of our home institutions. We thank Dr. M. Drees for a valuable discussion on the higher order QCD corrections for charm production. This work has been supported by the Japan Ministry of Education, Science, Culture, and Sports (Monbusho), the Japan Society for the Promotion of Science, the US Department of Energy, the US National Science Foundation, the Korean Science and Engineering Foundation, the Ministry of Education of Korea, and the Academia Sinica of the People's Republic of China.

## References

- [1] J.J. Sakurai and D. Schildknecht, Phys. Lett. **B40** (1972) 121.
- [2] S.J. Brodsky, T.A. DeGrand, J.F. Gunion, and J.H. Weis, Phys. Rev. Lett. **41** (1978) 672; Phys. Rev. **D19** (1979) 1418; H. Terazawa, J. Phys. Soc. Jpn. **47** (1979) 355; K. Kajantie and R. Raitio, Nucl. Phys. **B159** (1979) 528.
- [3] M. Drees and R.M. Godbole, Nucl. Phys. **B339** (1990) 355.
- [4] JADE Collab., W. Bartel et al., Phys. Lett. **B184** (1987) 288; TPC/2 $\gamma$  Collab., M. Alston-Garnjost et al., Phys. Lett. **B252** (1990) 499; TASSO Collab., W. Braunschweig et al., Z. Phys. **C47** (1990) 499.
- [5] AMY Collab., T. Aso et al., Phys. Lett. **B363** (1995) 249.
- [6] TOPAZ Collab., R. Enomoto et al., Phys. Rev. **D50** (1994) 1879.
- [7] TOPAZ Collab., R. Enomoto et al., Phys. Lett. **B328** (1994) 535.
- [8] TOPAZ Collab., M. Iwasaki et al., Phys. Lett. **B341** (1994) 99.
- [9] VENUS Collab., S. Uehara et al., Z. Phys. **C63** (1994) 213.
- [10] M. Drees, M. Krämer, J. Zunft, and P. M. Zerwas, Phys. Lett. **B306** (1993) 371.
- [11] HRS Collab., S. Abachi et al., Phys. Lett. **B205** (1988) 411; DELPHI Collab., P. Abreu et al., Phys. Lett. **B252** (1990) 140.
- [12] AMY Collab., T. Kumita et al., Phys. Rev. **D42** (1990) 1339; AMY Collab., Y. Sugimoto et al., Phys. Lett. **B369** (1996) 86.
- [13] M. Kuroda, Meiji Gakuin Univ. Research J. **27** (1988) 424.
- [14] H. Abramowicz, K. Charchula, and A. Levy, Phys. Lett. **B269** (1991) 458.
- [15] T. Sjöstrand, CERN-TH-6488-92(May 1992); T. Sjöstrand and M. Bengtsson, Comput. Phys. Commun. **43** (1987) 367.
- [16] Particle Data Group, Phys. Rev. **D50** (1994).
- [17] AMY Collab., R. Tanaka et al., Phys. Lett. **B277** (1992) 215; AMY Collab., B. J. Kim et al., Phys. Lett. **B325** (1994) 248.
- [18] JADE Collab., W. Bartel et al., Z.Phys. **C33** (1986) 23.
- [19] ALEPH Collab., D. Buskulic et al., Phys. Lett. **B355** (1995) 595.

## List of Figures

- 1 The  $\pi_s^\pm$  transverse momentum distribution obtained from simulated QPM Monte Carlo events. . . . . 9
- 2 The measured  $p_T^2$  distributions of soft-pion candidates with the result of fits. (a) The experimental data. The background curve is a fit of the function  $f_1$  with parameters determined from the Monte Carlo data. The normalization is performed for  $0.02 \leq p_T^2 \leq 0.08 \text{ GeV}^2/c^2$  ( $\chi^2/n.d.f. = 16/29$ ). (b) Simulated Monte Carlo results with  $D^{*+} \rightarrow D^0\pi^+$  decays excluded. The curve is a fit of the function  $f_1$  over the range  $0 \leq p_T^2 \leq 0.08 \text{ GeV}^2/c^2$  ( $\chi^2/n.d.f. = 31/37$ ). . . . . 10
- 3 The  $p_T^2$  distribution of soft-pion candidates with respect to the jet axis. The solid circles are the experimental data and the histograms are the NLO Monte Carlo calculation. The shaded histogram represents the contribution of  $D^{*+} \rightarrow D^0\pi^+$  decays obtained from the Monte Carlo simulated event sample. . . . . 11
- 4 Our measured  $e^+e^- \rightarrow e^+e^-D^{*\pm}X$  cross section together with previously reported results. The curves are the prediction of the Born level calculation (dotted line) and the direct plus resolved photon processes including NLO QCD corrections, where the parton distribution in the photon is taken from the LAC1 (solid line) and GRV (dashed line) models. The charm quark mass is taken to be  $1.6 \text{ GeV}/c^2$ . . . . . 12

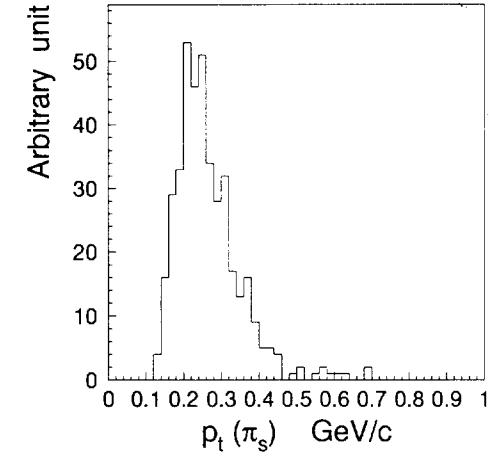


Fig. 1. The  $\pi_s^\pm$  transverse momentum distribution obtained from simulated QPM Monte Carlo events.

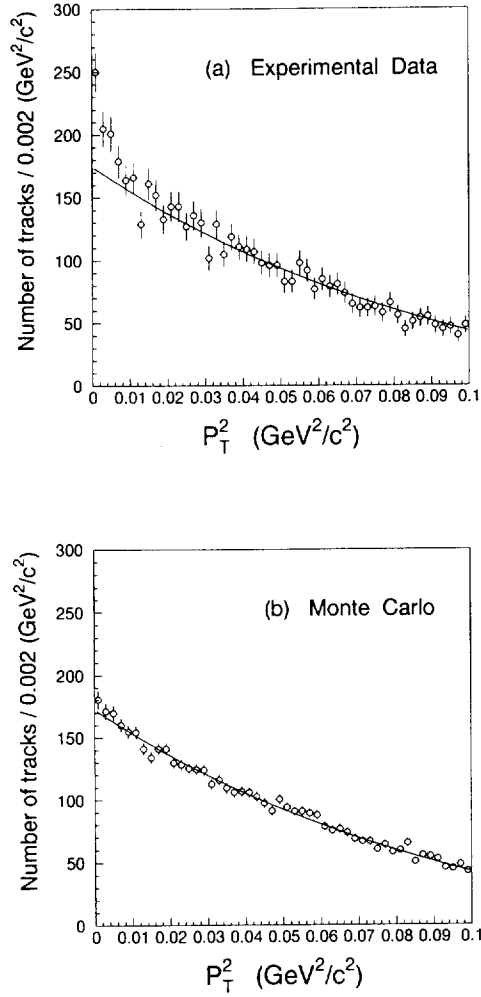


Fig. 2. The measured  $p_T^2$  distributions of soft-pion candidates with the result of fits. (a) The experimental data. The background curve is a fit of the function  $f_1$  with parameters determined from the Monte Carlo data. The normalization is performed for  $0.02 \leq p_T^2 \leq 0.08 \text{ GeV}^2/c^2$  ( $\chi^2/n.d.f. = 16/29$ ). (b) Simulated Monte Carlo results with  $D^{*+} \rightarrow D^0\pi^+$  decays excluded. The curve is a fit of the function  $f_1$  over the range  $0 \leq p_T^2 \leq 0.08 \text{ GeV}^2/c^2$  ( $\chi^2/n.d.f. = 31/37$ ).

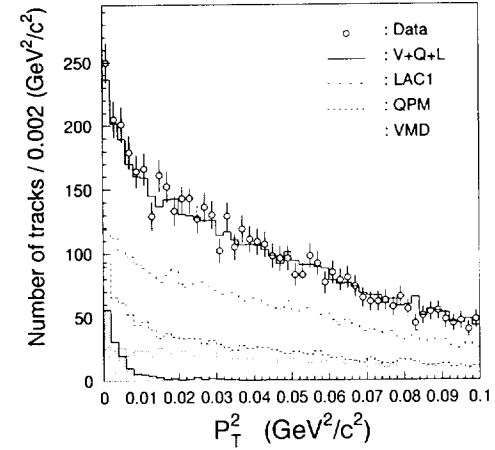


Fig. 3. The  $p_T^2$  distribution of soft-pion candidates with respect to the jet axis. The solid circles are the experimental data and the histograms are the NLO Monte Carlo calculation. The shaded histogram represents the contribution of  $D^{*+} \rightarrow D^0\pi^+$  decays obtained from the Monte Carlo simulated event sample.

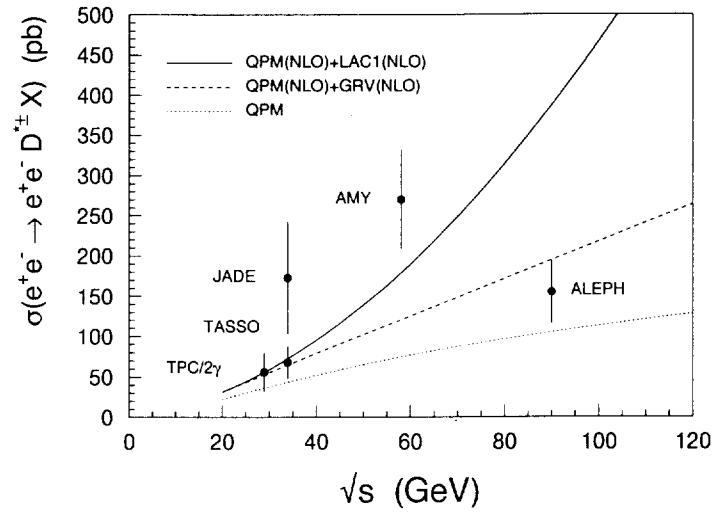


Fig. 4. Our measured  $e^+e^- \rightarrow e^+e^-D^{*\pm}X$  cross section together with previously reported results. The curves are the prediction of the Born level calculation (dotted line) and the direct plus resolved photon processes including NLO QCD corrections, where the parton distribution in the photon is taken from the LAC1 (solid line) and GRV (dashed line) models. The charm quark mass is taken to be  $1.6 \text{ GeV}/c^2$ .